RESEARCH ARTICLE

Carbodicarbene-Stibenium Ion-Mediated Functionalization of C(sp^3)–H and C(sp)–H Bonds

Levi Warring,[a] Karl S. Westendorff,[a],[c] Marc T. Bennett,[b] Kijeong Nam,[c] Brennan M. Stewart,[b] Diane A. Dickie,[b] Christopher Paolucci,*[c] T. Brent Gunnoe,*[b] Robert J. Gilliard*[a]

[a] Levi Warring, Karl Westendorff, Prof. Robert J. Gilliard
Department of Chemistry
Massachusetts Institute of Technology
77 Massachusetts Avenue, Cambridge, MA 02139, USA
E-mail: gilliard@mit.edu

[b] Marc T. Bennett, Brennan M. Stewart, Dr. Diane A. Dickie, Prof. T. Brent Gunnoe
Department of Chemistry
University of Virginia
409 McCormick Road, Charlottesville, VA 22904, USA.

[c] Karl Westendorff, Kijeong Nam, Prof. Christopher Paolucci
Department of Chemical Engineering
University of Virginia
385 McCormick Road, Charlottesville, VA 22904, USA.

Supporting information for this article is given via a link at the end of the document.

Abstract: Main-group element-mediated C–H activation remains experimentally challenging, and the development of clear concepts and design principles have been limited by the increased reactivity of relevant complexes, especially for the heavier elements. Herein, we report that the stibenium ion [(^{py}CDC)Sb][NTf$_2$]$_3$ (**1**) (^{py}CDC = bis-pyridyl carbodicarbene; NTf$_2$ = bis(trifluoromethanesulfonyl)imide) reacts with acetonitrile in the presence of the base 2,6-di-*tert*-butylpyridine to enable C(sp^3)–H bond breaking to generate the stiba-methylene nitrile complex [(^{py}CDC)Sb(CH$_2$CN)][NTf$_2$]$_2$ (**2**). Kinetic analyses were performed to elucidate the rate dependence for all the substrates involved in the reaction. Computational studies suggest that C–H activation proceeds via a mechanism in which acetonitrile first coordinates to the Sb center through the nitrogen atom in a κ^1 fashion, thereby weakening the C–H bond which can then be deprotonated by base in solution. Further, we show that **1** reacts with terminal alkynes in the presence of 2,6-di-*tert*-butylpyridine to enable C(sp)–H bond breaking to form stiba-alkynyl adducts of the type [(^{py}CDC)Sb(CCR)][NTf$_2$]$_2$ (**3a-f**). Compound **1** shows excellent specificity for the activation of the terminal C(sp)–H bond even across alkynes with diverse functionality. The resulting stiba-methylene nitrile and stiba-alkynyl adducts react with elemental iodine (I$_2$) to produce iodoacetonitrile and iodoalkynes, while regenerating an Sb trication.

Introduction

Targeted C–H bond activation is an invaluable tool used to insert carbon-carbon and carbon-heteroatom bonds in the synthesis of pharmaceuticals, natural products, and other high-value chemicals.[1] In contrast to transition-metal-mediated C–H activation, fewer examples of C–H bond breaking by main-group element complexes are known. This is in part due to inherent differences in the frontier molecular orbitals at play for bonding as well as their relative energies.[2] These differences in bonding are exacerbated for the heavier main-group elements, which have a decreased propensity for hybridization due to a mismatch in the size of the valence orbitals.[3] As a result, low-coordinate and low-oxidation state heavy main-group compounds are often reactive, making redox reactions significantly more challenging and difficult to control. Because of these challenges, our understanding of how to design main-group compounds to target C–H activation and functionalization is limited. Nonetheless, access to main-group compounds using uniquely crafted ligand and design strategies has enabled bond activations that were once reserved for their transition metal counterparts.[3a, 4]

One strategy that has been employed to construct main-group compounds that facilitate bond functionalization is to prepare highly Lewis acidic molecules for which a key step in the reaction is coordination of a substrate to the main-group element center.[5] Use of frustrated Lewis pairs (FLPs) has also been shown to be an effective means to activate many different types of bonds.[6] There are few examples of C–H bond breaking using highly Lewis acidic phosphenium ions,[7] and C–H bond breaking mediated by antimony and bismuth ions is even less common.[5e, 8] Despite this, the enhanced Lewis acidity of stibenium and bismuthenium ions compared to their lighter congeners makes them attractive targets to mediate bond activation.[9] We have found carbones to be excellent ligands that permit the stabilization of main-group Lewis acids.[10] In contrast to singlet carbenes,[11] carbones are capable of acting as two- or four-electron donors via

the two lone pairs of electrons at the central C(0) atom.[12] A special feature of carbones is that the additional electron density at carbon may manifest as a π-symmetric lone pair or participate in a donor-acceptor bond with a Lewis acidic partner. While its preference for employing one or both lone pairs depends on the identity of the main-group element and its orbital arrangements, both bonding situations typically result in increased stability compared to the analogous carbene complexes.[10a, 10b, 10e] We hypothesized that the electronic flexibility and enhanced stability provided by the carbones would be useful for the design of heavy main-group element complexes for C–H bond breaking.

Herein, we report carbodicarbene-stibenium ion-enabled functionalization of the C–H bonds of acetonitrile and terminal alkynes (Figure 1). This work exploits the reactivity of frustrated Lewis pairs, whereby the Lewis superacidic stibenium ion enables C(sp^3)–H and C(sp)–H deprotonation in the presence of a sterically encumbered base to form stiba-methylene nitrile and stiba-alkynyl adducts. In addition, we demonstrate the sequential reactivity of these adducts with elemental iodine to generate iodoacetonitrile and iodoalkynes. The reactions presented herein are among the first examples of a carbone-main-group element-mediated intermolecular bond functionalization.[7e, 13]

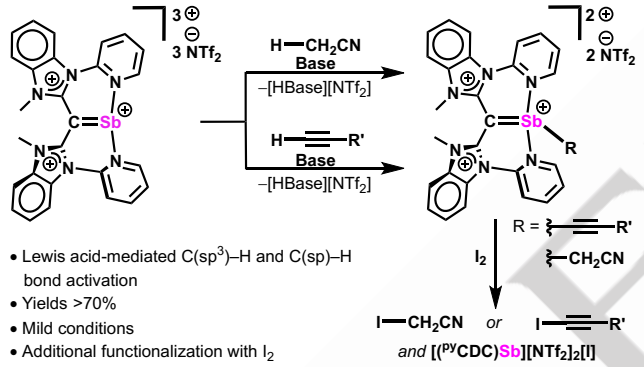

Figure 1. Carbodicarbene-stibenium ion-promoted C–H bond functionalization of acetonitrile and terminal alkynes and the subsequent functionalization of the resulting adducts with elemental iodine.

Results and Discussion

We selected the stibenium ion **1** as a compound of interest for potential C–H bond activation due to its high Gutmann-Beckett acceptor number (109) and Lewis superacidity, which is greater than its bismuth analog.[10f] Other reports have observed greater Lewis acidity for Sb compounds.[14] While screening for reactivity with arene substrates, we discovered that **1** reacts with CD_3CN in the presence of 2,6-di-*tert*-butylpyridine. Then, we reacted **1** with protio-acetonitrile (MeCN) and 2,6-di-*tert*-butylpyridine in 1,2-difluorobenzene (*o*DFB) at 95 °C (Scheme 1). After heating overnight (16 h), a yellow precipitate formed. The solid was collected to afford compound **2** in 73% isolated yield. The ^{1}H NMR spectrum of **2** shows two doublet resonances at 2.84 and 2.73 ppm ($^2J_{HH}$ ~ 17 Hz) corresponding to the diasterotopic methylene protons. The protons *ortho* to the pyridyl nitrogen atoms are shifted upfield (8.80 ppm) from **1** (8.98 ppm) in CD_3CN, and the *N*-methyl protons become inequivalent. The ^{13}C NMR spectrum shows the methylene (13.3 ppm) and nitrile carbon (119.6 ppm) resonances are shifted downfield from protio-acetonitrile (1.8 and 118.3 ppm).[15] The selection of 2,6-di-*tert*-butylpyridine as the base is important to achieve the formation of **2**. Namely, an organic base was selected that would be unlikely to coordinate to the Lewis acidic Sb atom but could deprotonate an Sb-activated C–H bond in a manner consistent with FLP-type chemistry.[16]

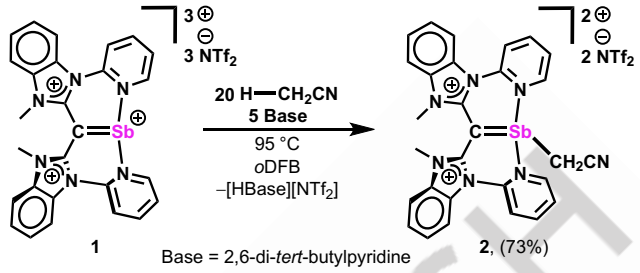

Scheme 1. Sb trication **1** activates MeCN to yield the Sb-cyanomethyl dication **2** in the presence of external base.

Single crystals of **2** suitable for X-ray diffraction studies were grown from a concentrated solution of *o*DFB (Figure 2). The ^{carbone}C–Sb bond length is 2.114(4) Å, which is slightly elongated compared to **1** (2.071(8) Å).[10f] The C28–Sb1 bond length of 2.209(4) Å is slightly longer than the sum of covalent radii for a C–Sb single bond (R(C–Sb) = 2.15 Å).[17] In contrast to **1**, weak coordination of the triflimide anions to Sb is not observed in the solid-state structure. To the best of our knowledge, compound **2** represents the first structurally characterized example of a stiba-methylene nitrile adduct.

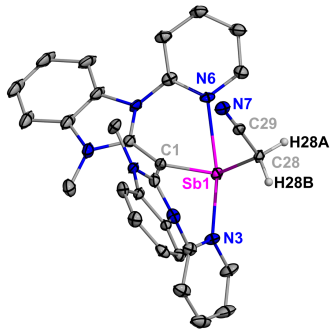

Figure 2. Molecular structure of **2**. Triflimide anions, disordered positions, and ^{py}CDC hydrogen atoms omitted for clarity. Thermal ellipsoids set at 30% probability. Bond lengths (Å) and angles (°): C1–Sb1: 2.114(4), C28–Sb1: 2.209(4), C28–C29: 1.438(6), C29–N7: 1.127(9), C1–Sb1–C28: 96.19(16), Sb1–C28–C29: 112.5(3).[18]

To gain insight into the mechanism for the reactivity of **1** with MeCN, a concentration versus time profile of the reaction of **1** with MeCN and 2,6-di-*tert*-butylpyridine was collected in 1,1,2,2-tetrachloroethane-d_2 (TCE-d_2) (Figure 3a). Plotting the natural log of product (i.e., **2**) concentration versus time results in an initial linear dependence (Figure S2), while the natural log of starting material concentration versus time maintains linearity (Figure 3b). Figure S2 shows the concentration of product **2** measured by ^{1}H NMR spectroscopy reaches a maximum at ~6 mM after 12 hours while ~8 mM of

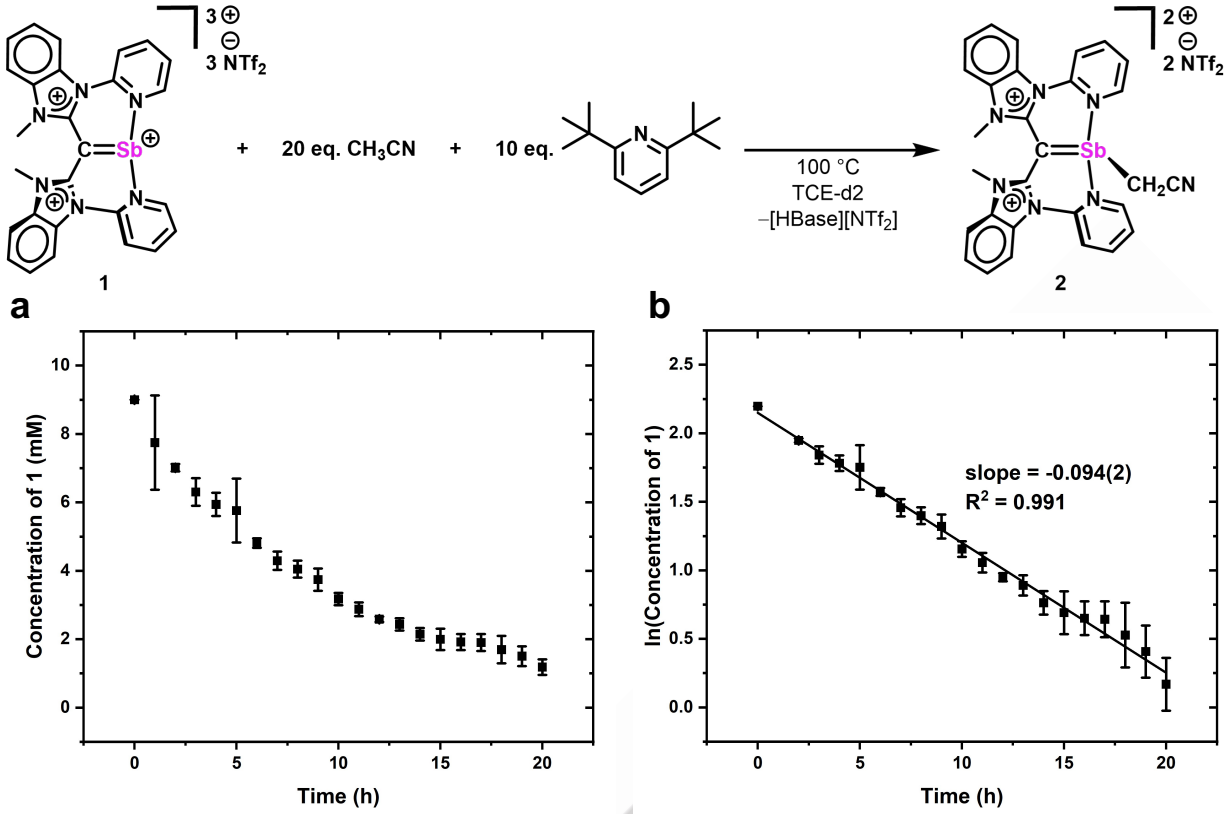

Figure 3. (**a**) Product concentration versus time and (**b**) natural log of concentration versus profiles for the reaction of **1** with MeCN in the presence of 2,6-di-*tert*-butylpyridine time. Reaction conditions: 0.4 mL TCE-d_2, 9 mM **1**, 20 equiv (relative to **1**) of MeCN, 10 equiv of 2,6-di-*tert*-butylpyridine. The data are based on a minimum of three replicate measurements with standard deviations shown.

starting material is consumed after 20 hours. The discrepancy between the consumption of **1** and formation of **2** is attributed to the partial solubility of the product in TCE-d_2. The linearity of the concentration of **1** versus time suggests that the reaction is first order with respect to the Sb trication.

Next, we conducted order studies on both the MeCN substrate and the 2,6-di-*tert*-butylpyridine base to better understand their role in the observed reactivity of **1**. The kinetic orders for acetonitrile and 2,6-di-*tert*-butylpyridine were determined by measuring the initial rates for the formation of product **2** (Figure 4). The initial rates obtained via ^{1}H NMR spectral monitoring vary linearly with acetonitrile concentration in the range 15 mM ≤ [MeCN] ≤ 360 mM. In the initial rates regime, the concentration versus time data are well-fit to linear regressions, and consistent rates are obtained when measuring the concentrations of **1** and **2**, suggesting that the solubility of **2** is not likely an issue at early reaction time points. A plot of log(k_{obs}) versus log[MeCN] (Figure 4a) gives a slope of 1.2(1), indicating that the reaction is likely first-order with respect to acetonitrile. Similarly, ^{1}H NMR spectral monitoring of 2,6-di-*tert*-butylpyridine concentration dependent studies in the range 3 mM ≤ [2,6-di-*tert*-butylpyridine] ≤ 360 mM gives linear regressions in the initial rate regime (Figure 4b). The logarithmic plot obtained gives a slope of 0.48(3). We attribute the slope of less-than-one to be a factor of labile coordination of the base to Sb, which likely impedes acetonitrile coordination at higher concentrations of 2,6-di-*tert*-butylpyridine, thus slowing the reaction rate.

To gain further insight into the reaction mechanism, we performed the reaction of **1** with MeCN or CD_3CN and 2,6-di-*tert*-butylpyridine in a 1:20:20 (**1**:MeCN/CD_3CN:base) molar mixture. After 90 minutes, a k_H/k_D (the ratio of the rate of reaction of protic-acetonitrile and deuterated-acetonitrile) of 6.1(7) was determined via ^{1}H NMR spectroscopy (Figure 4c). The k_H/k_D of 6.1(7) reflects a large primary kinetic isotope effect (KIE).

Given the preceding kinetic data, we considered two possible mechanisms for C–H activation and used density functional theory (DFT) calculations to evaluate the more favorable pathway. All calculations used the BP86 level of theory with GD3(BJ) empirical dispersion corrections, the def2-TZVPP basis set and its associated pseudopotentials for Sb, and the 6-31G(d,p) basis set for all other atoms. In the following calculations, we excluded all $[NTf_2]^-$ anions and balanced the charge on cationic Sb complexes with a uniform compensating background charge. Solvation free energies were calculated via the conductor-like polarizable continuum model (CPCM) model for tetrachloroethene as an approximation for the experimentally used 1,1,2,2-tetrachloroethane-d_2. Further computational details and rationale for our choice of functional, basis set, and solvation model are discussed in the Supporting Information.

We considered two pathways, analogous to those found in transition metal chemistry, which result in net C–H activation of

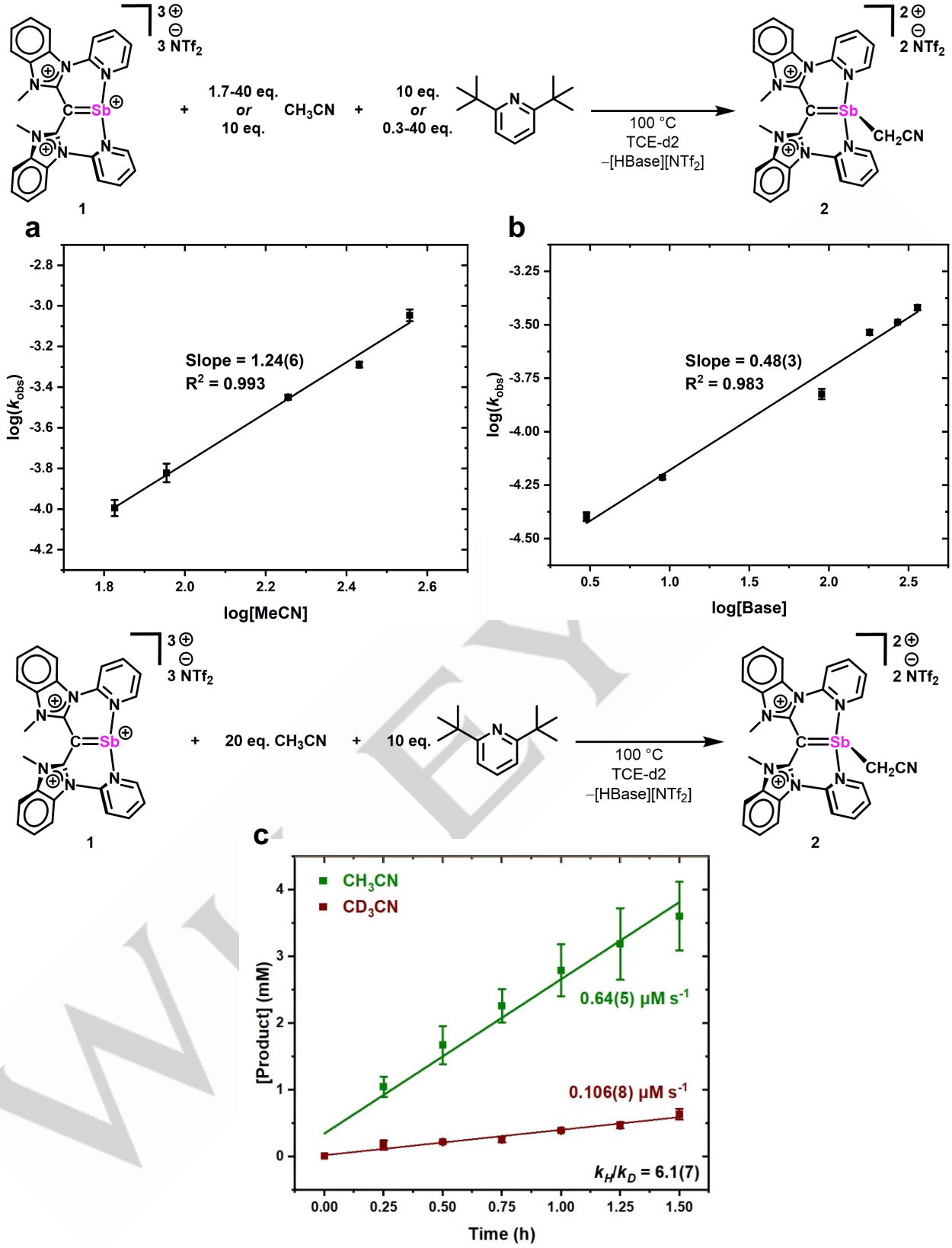

Figure 4. Acetonitrile (**a**) and 2,6-di-*tert*-butylpyridine (**b**) concentration dependence on rate of formation of **2**. Reaction conditions: 0.4 mL TCE-d_2, 100 °C, 9 mM **1**, 10 or x equivalents (relative to **1**) of MeCN, 10 or x equivalents of 2,6-di-*tert*-butylpyridine, and (**c**) Kinetic isotope effect for the reaction of compound **1** with MeCN/CD_3CN and base. Reaction conditions: 0.4 mL TCE-d_2, 9 mM **1**, 20 equivalents (relative to **1**) of MeCN or MeCN-d_3, 20 equivalents of 2,6-di-*tert*-butylpyridine. The data are based on a minimum of three replicate measurements with standard deviations shown.

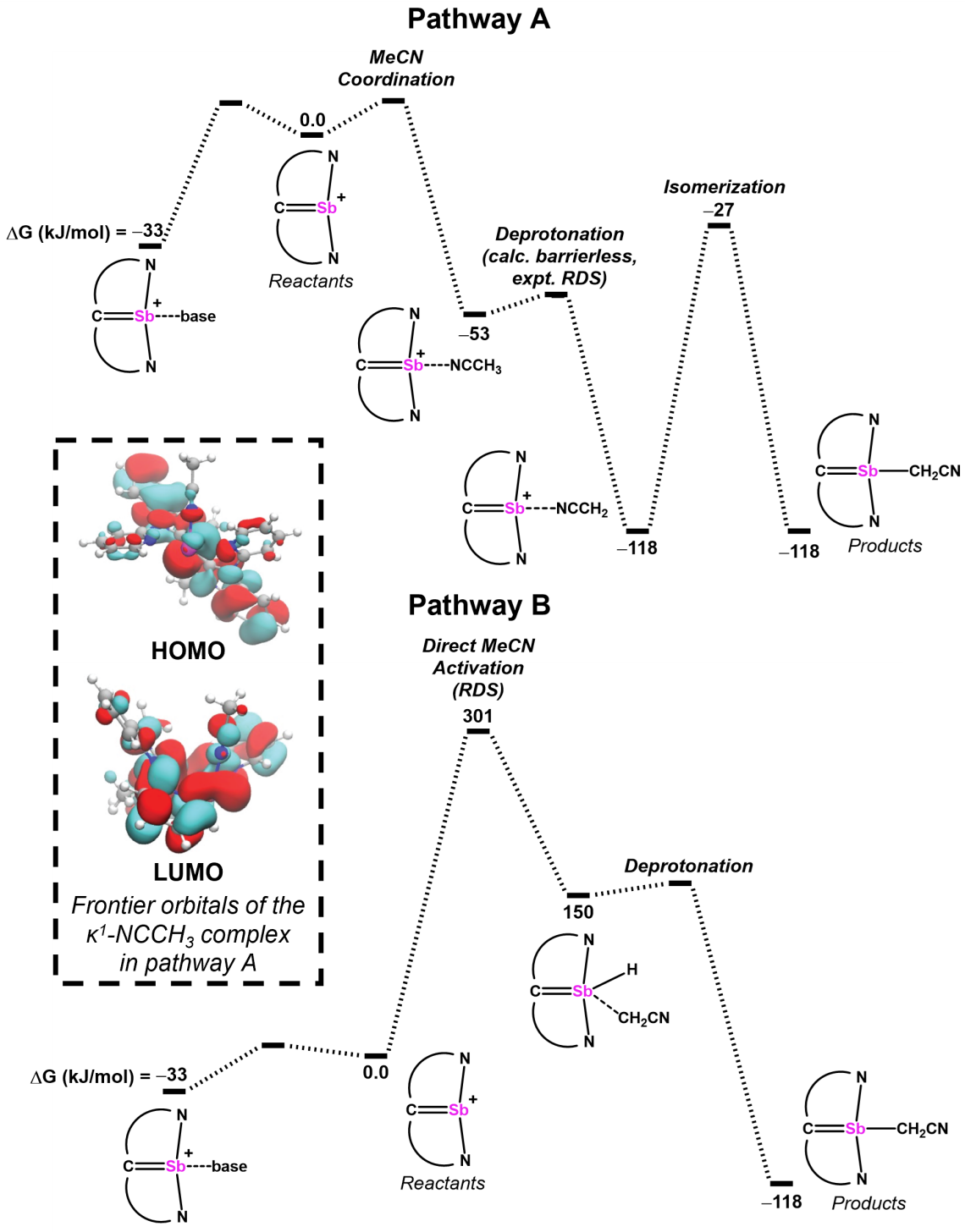

Figure 5. Two possible pathways resulting in net C–H activation of acetonitrile with complex **1**. In pathway A, the Sb complex coordinates acetonitrile in a κ^1 fashion, after which it is deprotonated by base and isomerizes to form complex **2**. In pathway B, the Sb complex directly activates the acetonitrile C–H bond and base deprotonates the resulting Sb complex to form complex **2**.

the MeCN bond across the Sb center. In pathway A, MeCN is bound to complex **1** in a k^1 fashion, after which 2,6-di-*tert*-butylpyridine deprotonates the MeCN ligand and the carbanion ligand isomerizes to form complex **2** (Figure 5). In pathway B, a MeCN C–H bond is directly coordinated by complex **1**, after which the Sb–H complex is deprotonated by 2,6-di-*tert*-butylpyridine to form complex **2** (Figure 5).

Pathway A shows that k^1 coordination of MeCN to complex **1** (Figure 5, inset) has a binding free energy of –53 kJ/mol relative to dissociated complex **1** and MeCN, and coordination of 2,6-di-*tert*-butylpyridine has a reaction energy of –33 kJ/mol. ^{1}H NMR spectroscopic analysis of a TCE-d_2 solution of **1** and MeCN shows that the resonance corresponding to MeCN is shifted slightly downfield from its expected chemical shift, indicating potential

coordination of the nitrile to Sb (Figure S45). Conversely, a solution of **1** and 2,6-di-*tert*-butylpyridine reveals no notable changes in chemical shift, suggesting that there is substantial steric repulsion between the molecules. Subsequent deprotonation of the k^1 bound MeCN ligand has a reaction energy of –65 kJ/mol, and isomerization of the carbanion to form complex **2** has a barrier of 91 kJ/mol and a reaction energy of –1 kJ/mol. In contrast to the low barriers computed in pathway A, pathway B had a concerted C–H activation barrier of +301 kJ/mol and a reaction energy of +150 kJ/mol relative to the dissociated Sb complex and MeCN. Subsequent deprotonation of the Sb complex by 2,6-di-*tert*-butylpyridine has a reaction energy of –267 kJ/mol. Though these calculations suggest that pathway A is favored due to its lower calculated barrier, the unknown explicit solvent structure around the active site, the many possible proton donor/acceptor species in the rate-determining step (RDS), and the potential non-adiabaticity of the protonation/deprotonation step prevent the unambiguous identification of the RDS via the calculations employed here.[19] Therefore, to determine whether the deprotonation step was rate-controlling in the observed reaction, we experimentally measured the reaction with another organic base of a different strength. Using lutidine, which is a stronger Lewis base than the original 2,6-di-*tert*-butylpyridine,[20] the reaction proceeds instantaneously at room temperature. Moreover, use of the sterically comparable but stronger Lewis base 2,4,6-tri-*tert*-butylpyridine leads to > 90% conversion to **2** after 2 hours (at 100 °C), which is approximately ten times faster than using 2,6-di-*tert*-butylpyridine. These results suggest that deprotonation of **1** is likely the rate-controlling step in the reaction sequence. Given that direct C–H activation, a step that does not depend on the base strength, is the rate-determining step in pathway B, pathway A is most consistent with these results.

Rate law derivations for pathway A (see Supporting Information, pages S41-42) agree with the **1** and MeCN concentration order studies as well as the base concentration order experiments assuming that base competitively binds to **1** in solution with MeCN, as suggested by the computations. Further, the RDS of the reaction involves a proton transfer, in agreement with the experimentally observed KIE. While these data are also consistent with a mechanism that follows pathway B where the RDS is deprotonation of the Sb center, the barrier to deprotonation would have to exceed 154 kJ/mol relative to the activated Sb MeCN complex and free base, which would prevent the reaction from proceeding rapidly at room temperature with lutidine as the base. The combined experimental and computational data suggest that the C(sp^3)–H activation of MeCN is driven by the acidity of the MeCN C–H bond upon coordination to Sb and the acceptor base.

With this understanding, we attempted to react **1** with two terminal alkynes. We posited that the alkyne moiety could coordinate to the Lewis acidic antimony center, enabling deprotonation of the more acidic C–H bonds at the terminal position (relative to acetonitrile). Compound **1** reacts with (trimethylsilyl)acetylene or phenylacetylene in the presence of 2,6-di-*tert*-butylpyridine in *o*DFB to form the stiba-alkynyl adducts **3a** and **3b** in excellent yields (Scheme 2). Similar to the reaction of **1** with MeCN, two *N*-methyl resonances are observed after

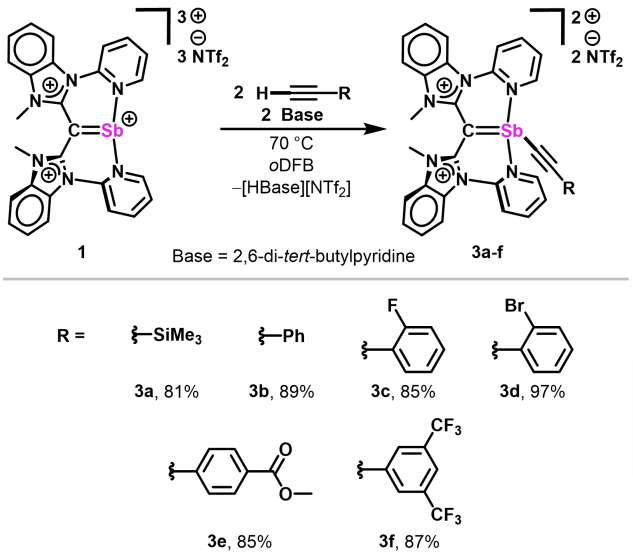

Scheme 2. Reaction of **1** with terminal alkynes and base to afford stibaalkynyl dications **3a-f**. Isolated yields are shown.

the reaction of **1** with the terminal alkynes, indicating a loss of chemical equivalency from the starting complex. ^{1}H NMR spectroscopy analysis of **3a** shows a singlet resonance at –0.34 ppm in CD_3CN corresponding to the trimethylsilyl protons, which is shifted upfield from the unreacted alkyne (0.19 ppm). Further, the ^{1}H-^{29}Si HMQC spectrum of **3a** shows a broad singlet resonance at –17.3 ppm, indicating a singular Si environment corresponding to the alkynyl adduct. Given the quantitative conversion of compound **1** to **3a** and **3b**, we expanded the scope of terminal alkynes to test for tolerance of more diverse functional groups. Addition of **1** to a solution of 2 equivalents of both the terminal alkyne and 2,6-di-*tert*-butylpyridine leads to nearly quantitative conversion to the stiba-alkynyl adducts **3c-f** based on analysis by ^{1}H NMR spectroscopy. Reaction progress was monitored by the formation of resonances corresponding to protonated base, which forms in an equimolar ratio to the stiba-alkynyl adducts (see Supporting Information). The formation of compounds **3c** and **3f** was also monitored using ^{19}F NMR spectroscopy (singlet resonances at –111.5 ppm and –63.7 ppm, respectively). Despite significant effort, attempts to isolate single crystals of **3a-f** were unsuccessful.[21]

We observed that **2** reacts with I_2 to form iodoacetonitrile and the proposed Sb trication **4** in full conversion by ^{1}H NMR spectroscopic analysis (Scheme 3). Notably, ^{1}H NMR spectroscopy shows the loss of the two doublets corresponding to the methylene protons at 2.84 and 2.73 ppm and the appearance of a new singlet resonance at 3.64 ppm in CD_3CN that corresponds to iodoacetonitrile. Additionally, the ^{13}C NMR spectrum shows the methylene carbon resonance is shifted significantly upfield from 13.3 ppm to –29.8 ppm. The inequivalent *N*-methyl groups from **2** become equivalent upon formation of compound **4**, which presumably contains two $[NTf_2]^-$ anions and one $[I]^-$ anion.

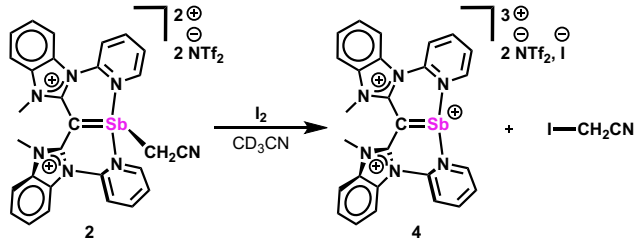

Scheme 3. Synthesis of iodoacetonitrile from Sb-cyanomethyl dication **2** upon reaction with elemental iodine.

Given the versatility of haloalkynes as synthetic building blocks,[22] we also demonstrated the reactivity of the stiba-alkynyl adducts **3a-f** with I_2 to form 1-iodo-alkynes while also generating the Sb trication **4** (Scheme 4). The addition of I_2 to compound **3a** leads to full conversion to **4** and 1-iodo-2-(trimethylsilyl)acetylene by ^{1}H NMR spectroscopic analysis. There is a downfield shift in the ^{1}H NMR spectrum for the trimethylsilyl protons from –0.34 ppm to 0.15 ppm in CD_3CN. Concomitantly, the two singlet *N*-methyl proton resonances at 3.35 and 3.21 ppm for **3a** become equivalent upon addition of I_2, indicating loss of the alkynyl moiety from Sb and formation of **4**. Compounds **3b-f** react in the same manner as **3a** with I_2, generating **4** and their respective 1-iodo-alkyne. The formation of 1-iodoalkynes was confirmed by high-resolution mass spectrometry and ^{1}H NMR spectroscopy. Iodination of terminal alkynes has traditionally been achieved using late transition metal catalysts, strong bases, or by using organolithium reagents, which can limit the functional group diversity of the alkyne.[23]

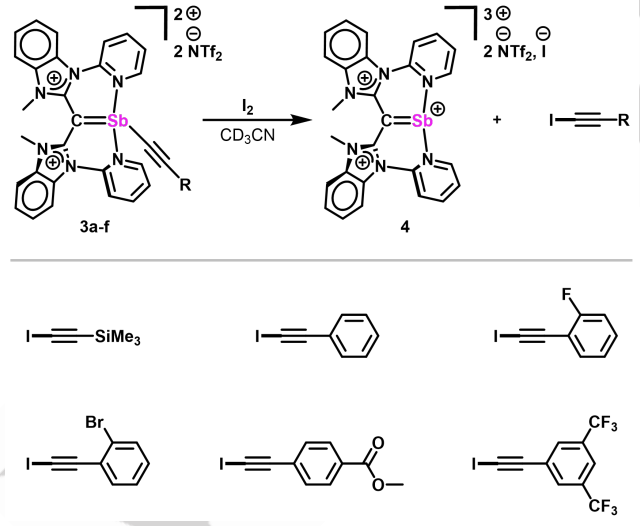

Scheme 4. Synthesis of iodoalkynes from Sb-alkynyl dications.

Conclusion

We demonstrate the C–H functionalization of acetonitrile and terminal alkynes using a carbodicarbene-stibenium ion. The Lewis superacidic stibenium trication reacts with acetonitrile in the presence of 2,6-di-*tert*-butylpyridine to form a stiba-methylene nitrile adduct, and both mechanistic and computational studies support a mechanism where acetonitrile first coordinates to the Sb center in a k^1 fashion, thereby increasing the acidity of its C–H bonds which can then be subsequently deprotonated. The resulting stiba-methylene nitrile adduct is susceptible to reactivity with electrophilic substrates. We also show that the stibenium trication enables the functionalization of the C(sp)–H bond in terminal alkynes to form stiba-alkynyl adducts that readily react with iodine to form iodo-alkynes in quantitative conversion. We demonstrate a wide range of functional group tolerance for the iodination of terminal alkynes. This work represents some of the first reactivity studies of carbone-heavy group 15 element cations, which we hope to expand on in future reports.

Supporting Information

The authors have cited additional references within the Supporting Information.[10f, 24]

Acknowledgements

We are grateful to the Massachusetts Institute of Technology (M.I.T.) and the University of Virginia (UVA). This work was supported by the donors of ACS Petroleum Research Fund under Doctoral New Investigator Grant 62280-DNI3. R.J.G. served as Principal Investigator on ACS PRF 62280-DNI3 that provided support for L.S.W. Support for the efforts of MTB and TBG came from the U.S. National Science Foundation under award CHE-2102433. Single-crystal X-ray diffraction experiments were performed on a diffractometer at the University of Virginia funded by the NSF-MRI program (CHE-2018870).

Keywords: Carbones, Antimony, Cations, Hydrocarbons, Reactivity

[1] a) U. Dutta, S. Maiti, T. Bhattacharya, D. Maiti, *Science* **2021**, *372*, eabd5992; b) L. McMurray, F. O'Hara, M. J. Gaunt, *Chem. Soc. Rev.* **2011**, *40*, 1885-1898; c) J. Yamaguchi, A. D. Yamaguchi, K. Itami, *Angew. Chem., Int. Ed.* **2012**, *51*, 8960-9009; d) J. Wencel-Delord, F. Glorius, *Nat. Chem.* **2013**, *5*, 369-375.

[2] H. B. Wedler, P. Wendelboe, P. P. Power, *Organometallics* **2018**, *37*, 2929-2936.

[3] a) P. P. Power, *Nature* **2010**, *463*, 171-177; b) P. T. Wolczanski, *Organometallics* **2024**, *43*, 787-801.

[4] a) I. J. Casely, J. W. Ziller, M. Fang, F. Furche, W. J. Evans, *J. Am. Chem. Soc.* **2011**, *133*, 5244-5247; b) T. Tsuruta, D. Spinnato, H. W. Moon, M. Leutzsch, J. Cornella, *J. Am. Chem. Soc.* **2023**, *145*, 25538-25544; c) O. Planas, F. Wang, M. Leutzsch, J. Cornella, *Science* **2020**, *367*, 313-317; d) H. W. Moon, J. Cornella, *ACS Catal.* **2022**, *12*, 1382-1393; e) X. Yang, E. J. Reijerse, K. Bhattacharyya, M. Leutzsch, M. Kochius, N. Nöthling, J. Busch, A. Schnegg, A. A. Auer, J. Cornella, *J. Am. Chem. Soc.* **2022**, *144*, 16535-16544; f) O. Planas, V. Peciukenas, J. Cornella, *J. Am. Chem. Soc.* **2020**, *142*, 11382-11387; g) K. L. Mears, G.-A. Nguyen, B. Ruiz, A. Lehmann, J. Nelson, J. C. Fettinger, H. M. Tuononen, P. P. Power, *J. Am. Chem. Soc.* **2024**; h) S. Ni, D. Spinnato, J. Cornella, *J. Am. Chem. Soc.* **2024**; i) V. Kumar, R. G. Gonnade, C. B. Yildiz, M. Majumdar, *Angew. Chem.* **2021**, *133*, 25726-25733.

[5] a) M. Hirai, J. Cho, F. P. Gabbaï, *Chem.—Eur. J.* **2016**, *22*, 6537-6541; b) R. A. Ugarte, D. Devarajan, R. M. Mushinski, T. W. Hudnall, *Dalton Trans.* **2016**, *45*, 11150-11161; c) M. Yang, M. Hirai, F. P. Gabbaï, *Dalton Trans.* **2019**, *48*, 6685-6689; d) M. Yang, N. Pati, G. Bélanger-Chabot, M. Hirai, F. P. Gabbaï, *Dalton Trans.* **2018**, *47*, 11843-11850; e) R. Qiu, S. Yin, X. Zhang, J. Xia, X. Xu, S. Luo, *Chem. Commun.* **2009**, 4759-4761; f) P. Ondet, G. Lemière, E. Duñach, *Eur. J. Org. Chem.* **2017**, *2017*, 761-780; g) S. C. T. Erick Lopez, Ram S. Mohan, *Polyhedron* **2022**, *222*; h) J. M. Lipshultz, G. Li, A. T. Radosevich, *J. Am. Chem. Soc.* **2021**, *143*, 1699-1721; i) T. J. Hannah, W. M. McCarvell, T. Kirsch, J. Bedard, T. Hynes, J. Mayho, K. L. Bamford, C. W. Vos, C. M. Kozak, T. George, J. D. Masuda, S. S. Chitnis, *Chem. Sci.* **2023**, *14*, 4549-4563; j) S. Balasubramaniam, S. Kumar, A. P. Andrews, B. Varghese, E. D. Jemmis, A. Venugopal, *Eur. J. Inorg. Chem.* **2019**, 3265-3269; k) J. Zhang, J. Wei, W.-Y. Ding, S. Li, S.-H. Xiang, B. Tan, *J. Am. Chem. Soc.* **2021**, *143*, 6382-6387; l) X. Lan, X. Zhang, Y. Mei, C. Hu, L. L. Liu, *Dalton Trans.* **2023**.

[6] a) D. W. Stephan, *Science* **2016**, *354*, aaf7229; b) J. Krieft, P. C. Trapp, Y. V. Vishnevskiy, B. Neumann, H.-G. Stammler, J.-H. Lamm, N. W. Mitzel, *Chem. Sci.* **2024**, *15*, 12118-12125; c) J. Krieft, B. Neumann, H.-G. Stammler, N. W. Mitzel, *Dalton Trans.* **2024**, *53*, 11762-11768; d) A. R. Jupp, D. W. Stephan, *Trends in Chemistry* **2019**, *1*, 35-48.

[7] a) M. H. Holthausen, J. M. Bayne, I. Mallov, R. Dobrovetsky, D. W. Stephan, *J. Am. Chem. Soc.* **2015**, *137*, 7298-7301; b) D. Roth, J. Stirn, D. W. Stephan, L. Greb, *J. Am. Chem. Soc.* **2021**, *143*, 15845-15851; c) D. Roth, A. T. Radosevich, L. Greb, *J. Am. Chem. Soc.* **2023**, *145*, 24184-24190; d) A. Kroll, H. Steinert, M. Jörges, T. Steinke, B. Mallick, V. H. Gessner, *Organometallics* **2020**, *39*, 4312-4319; e) N. Đorđević, R. Ganguly, M. Petković, D. Vidović, *Inorg. Chem.* **2017**, *56*, 14671-14681.

[8] a) G. A. Olah, R. H. Schlosberg, *J. Am. Chem. Soc.* **1968**, *90*, 2726-2727; b) L. Capaldo, M. Ertl, M. Fagnoni, G. Knör, D. Ravelli, *ACS Catal.* **2020**, *10*, 9057-9064; c) B. Ritschel, J. Poater, H. Dengel, F. M. Bickelhaupt, C. Lichtenberg, *Angew. Chem., Int. Ed.* **2018**, *57*, 3825-3829; d) K. Oberdorf, A. Hanft, X. Xie, F. M. Bickelhaupt, J. Poater, C. Lichtenberg, *Chem. Sci.* **2023**, *14*, 5214-5219; e) R. Wang, S. Martínez, J. Schwarzmann, C. Z. Zhao, J. Ramler, C. Lichtenberg, Y.-M. Wang, *J. Am. Chem. Soc.* **2024**.

[9] a) L. T. Maltz, F. P. Gabbaï, *Inorg. Chem.* **2023**, *62*, 13566-13572; b) B. L. Murphy, F. P. Gabbaï, *J. Am. Chem. Soc.* **2023**, *145*, 19458-19477; c) M. Baaz, V. Gutmann, O. Kunze, *Monatshefte für Chemie und verwandte Teile anderer Wissenschaften* **1962**, *93*, 1142-1161.

[10] a) C.-L. Deng, A. D. Obi, B. Y. E. Tra, S. K. Sarkar, D. A. Dickie, R. J. Gilliard, *Nat. Chem.* **2024**, *16*, 437-445; b) K. K. Hollister, A. Molino, G. Breiner, J. E. Walley, K. E. Wentz, A. M. Conley, D. A. Dickie, D. J. D. Wilson, R. J. Gilliard, *J. Am. Chem. Soc.* **2022**, *144*, 590-598; c) A. D. Obi, C.-L. Deng, A. J. Alexis, D. A. Dickie, R. J. Gilliard, *Chem. Commun.* **2024**, *60*, 1880-1883; d) A. D. Obi, D. A. Dickie, W. Tiznado, G. Frenking, S. Pan, R. J. Gilliard, Jr., *Inorg. Chem.* **2022**, *61*, 19452-19462; e) J. Walley, L. Warring, G. Wang, D. A. Dickie, S. Pan, G. Frenking, R. J. Gilliard, *Angew. Chem., Int. Ed.* **2021**, *60*, 6682-6690; f) L. S. Warring, J. E. Walley, D. A. Dickie, W. Tiznado, S. Pan, R. J. Gilliard, *Inorg. Chem.* **2022**, *61*, 18640-18652.

[11] a) V. Nesterov, D. Reiter, P. Bag, P. Frisch, R. Holzner, A. Porzelt, S. Inoue, *Chem. Rev.* **2018**, *118*, 9678-9842; b) M. Soleilhavoup, G. Bertrand, *Acc. Chem. Res.* **2015**, *48*, 256-266; c) D. Munz, *Organometallics* **2018**, *37*, 275-289; d) S. Kumar Kushvaha, A. Mishra, H. W. Roesky, K. Chandra Mondal, *Chem. Asian J.* **2022**, *17*, e202101301.

[12] a) C. A. Dyker, V. Lavallo, B. Donnadieu, G. Bertrand, *Angew. Chem., Int. Ed.* **2008**, *47*, 3206-3209; b) F. Ramirez, N. B. Desai, B. Hansen, N. McKelvie, *J. Am. Chem. Soc.* **1961**, *83*, 3539-3540; c) R. Tonner, G. Frenking, *Angew. Chem., Int. Ed.* **2007**, *46*, 8695-8698; d) W.-C. Chen, Y.-C. Hsu, C.-Y. Lee, G. P. A. Yap, T.-G. Ong, *Organometallics* **2013**, *32*, 2435-2442; e) W.-C. Chen, J.-S. Shen, T. Jurca, C.-J. Peng, Y.-H. Lin, Y.-P. Wang, W.-C. Shih, G. P. A. Yap, T.-G. Ong, *Angew. Chem., Int. Ed.* **2015**, *54*, 15207-15212; f) Y.-C. Hsu, J.-S. Shen, B.-C. Lin, W.-C. Chen, Y.-T. Chan, W.-M. Ching, G. P. A. Yap, C.-P. Hsu, T.-G. Ong, *Angew. Chem.* **2015**, *127*, 2450-2454; g) B. S. Aweke, C.-H. Yu, J.-S. Shen, S. Wang, G. P. A. Yap, W.-C. Chen, T.-G. Ong, *Inorg. Chem.* **2023**, *62*, 12664-12673; h) T. Koike, J.-K. Yu, M. M. Hansmann, *Science* **2024**, *385*, 305-311.

[13] a) K. Chulsky, I. Malahov, D. Bawari, R. Dobrovetsky, *J. Am. Chem. Soc.* **2023**, *145*, 3786-3794; b) M. Q. Y. Tay, Y. Lu, R. Ganguly, D. Vidović, *Chem.—Eur. J.* **2014**, *20*, 6628-6631.

[14] a) D. Sharma, S. Balasubramaniam, S. Kumar, E. D. Jemmis, A. Venugopal, *Chem. Commun.* **2021**, *57*, 8889-8892; b) G. Park, D. J. Brock, J.-P. Pellois, F. P. Gabbaï, *Chem* **2019**, *5*, 2215-2227.

[15] G. R. Fulmer, A. J. M. Miller, N. H. Sherden, H. E. Gottlieb, A. Nudelman, B. M. Stoltz, J. E. Bercaw, K. I. Goldberg, *Organometallics* **2010**, *29*, 2176-2179.

[16] a) M. A. Dureen, D. W. Stephan, *J. Am. Chem. Soc.* **2009**, *131*, 8396-8397; b) M. A. Dureen, C. C. Brown, D. W. Stephan, *Organometallics* **2010**, *29*, 6594-6607; c) P. Vasko, I. A. Zulkifly, M. Á. Fuentes, Z. Mo, J. Hicks, P. C. J. Kamer, S. Aldridge, *Chem.—Eur. J.* **2018**, *24*, 10531-10540; d) J. Leitl, A. R. Jupp, E. R. M. Habraken, V. Streitferdt, P. Coburger, D. J. Scott, R. M. Gschwind, C. Müller, J. C. Slootweg, R. Wolf, *Chem.—Eur. J.* **2020**, *26*, 7788-7800; e) D. W. Stephan, *J. Am. Chem. Soc.* **2015**, *137*, 10018-10032; f) A. Brar, S. Mummadi, D. K. Unruh, C. Krempner, *Organometallics* **2020**, *39*, 4307-4311.

[17] P. Pyykkö, *J. Phys. Chem. A* **2015**, *119*, 2326-2337.

[18] CCDC 2365988 (2) contains the supplementary crystallographic data for this paper. These data can be obtained free of charge via www.ccdc.cam.ac.uk/data_request/cif, or by emailing data_request@ccdc.cam.ac.uk, or by contacting The Cam-bridge Crystallographic Data Centre, 12 Union Road,Cambridge CB2 1EZ, UK; fax: +44 1223 336033.

[19] G. Norjmaa, G. Ujaque, A. Lledós, *Topics in Catalysis* **2022**, *65*, 118-140.

[20] E. Follet, H. Zipse, S. Lakhdar, A. R. Ofial, G. Berionni, *Synthesis* **2017**, *49*, 3495-3504.

[21] In the work-up of the reaction mixtures of the syntheses of 3a-f, sodium hydride is added to the solution to deprotonate 1H-2,6-di-tert-butylpyridium triflimide. Due to similar solubities, other methods of separating 3a-f from the protonated base were not successful, which we hypothesized was inhibiting growth of single crystals. However, even purified samples of 3a-f did not afford crystals after numerous crystallization attempts.

[22] W. Wu, H. Jiang, *Acc. Chem. Res.* **2014**, *47*, 2483-2504.

[23] a) G. Pelletier, S. Lie, J. J. Mousseau, A. B. Charette, *Org. Lett.* **2012**, *14*, 5464-5467; b) J. Yan, J. Li, D. Cheng, *Synlett* **2007**, *2007*, 2442-2444; c) P. Michel, A. Rassat, *Tetrahedron Lett.* **1999**, *40*, 8579-8581; d) S. Chen, X. Zhang, H. Zhao, X. Guo, X. Hu, *Chin. J. Org. Chem.* **2018**, *38*, 1172.

[24] a) Y.-C. Hsu, J.-S. Shen, B.-C. Lin, W.-C. Chen, Y.-T. Chan, W.-M. Ching, G. P. A. Yap, C.-P. Hsu, T.-G. Ong, *Angew. Chem., Int. Ed.* **2015**, *54*, 2420-2424; b) Bruker. *APEX4.* Bruker AXS Inc.; Madison, WI, USA: 2021; c) L. Krause, R. Herbst-Irmer, G. M. Sheldrick, D. Stalke, *Journal of Applied Crystallography* **2015**, *48*, 3-10; d) G. M. Sheldrick, *Acta Crystallographica Section A* **2015**, *71*, 3-8; e) O. V. Dolomanov, L. J. Bourhis, R. J. Gildea, J. A. K. Howard, H. Puschmann, *Journal of Applied Crystallography* **2009**, *42*, 339-341; f) J. P. Perdew, *Physical Review B* **1986**, *33*, 8822-8824; g) A. D. Becke, *Physical Review A* **1988**, *38*, 3098-3100; h) S. Grimme, S. Ehrlich, L. Goerigk, *J. Comput. Chem.* **2011**, *32*, 1456-

1465; i) D. E. Woon, T. H. Dunning, Jr., *J. Chem. Phys.* **1993**, *98*, 1358-1371; j) R. A. Kendall, T. H. Dunning, Jr., R. J. Harrison, *J. Chem. Phys.* **1992**, *96*, 6796-6806; k) M. J. Frisch, G. W. Trucks, H. B. Schlegel, G. E. Scuseria, M. A. Robb, J. R. Cheeseman, G. Scalmani, V. Barone, G. A. Petersson, H. Nakatsuji, X. Li, M. Caricato, A. V. Marenich, J. Bloino, B. G. Janesko, R. Gomperts, B. Mennucci, H. P. Hratchian, J. V. Ortiz, A. F. Izmaylov, J. L. Sonnenberg, Williams, F. Ding, F. Lipparini, F. Egidi, J. Goings, B. Peng, A. Petrone, T. Henderson, D. Ranasinghe, V. G. Zakrzewski, J. Gao, N. Rega, G. Zheng, W. Liang, M. Hada, M. Ehara, K. Toyota, R. Fukuda, J. Hasegawa, M. Ishida, T. Nakajima, Y. Honda, O. Kitao, H. Nakai, T. Vreven, K. Throssell, J. A. Montgomery Jr., J. E. Peralta, F. Ogliaro, M. J. Bearpark, J. J. Heyd, E. N. Brothers, K. N. Kudin, V. N. Staroverov, T. A. Keith, R. Kobayashi, J. Normand, K. Raghavachari, A. P. Rendell, J. C. Burant, S. S. Iyengar, J. Tomasi, M. Cossi, J. M. Millam, M. Klene, C. Adamo, R. Cammi, J. W. Ochterski, R. L. Martin, K. Morokuma, O. Farkas, J. B. Foresman, D. J. Fox. *Gaussian 16 Rev. C.01*. Wallingford, CT: 2016; l) R. C. Weast, *CRC, Handbook of Chemistry and Physics, ed., 76th edn.*, CRC Press Inc.,Boca Raton, FL, United States, **1995**; m) M. H. Abraham, J. Andonian-Haftvan, G. S. Whiting, A. Leo, R. S. Taft, *J. Chem. Soc., Perkin Trans. 2* **1994**, 1777-1791.

Entry for the Table of Contents

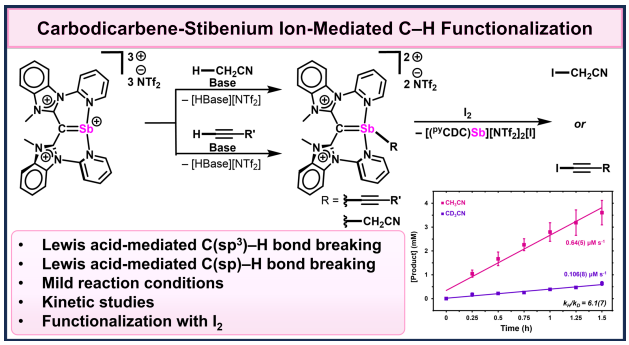

A Lewis acidic carbodicarbene-stibenium ion mediates C(sp^3)–H and C(sp)–H bond breaking of acetonitrile and terminal alkynes in the presence of an organic base. The resulting adducts can be reacted with elemental iodine to functionalize these C–H bonds in stoichiometric fashion.